Sādhanā (2020)45:113
https://doi.org/10.1007/s12046-020-01349-7

Statistical modeling of rubberized concrete beams confined by FRP using RSM technique

RANA FAISAL TUFAIL[1,*], XIONG FENG[2], MUHAMMAD ZAHID[3], NODIR UTASHEV[4], TAHIR MEHMOOD[1], ADNAN NAWAZ[1], AHSEN MAQSOOM[1] and HAMMAD SALAHUDDIN[1]

[1]Department of Civil Engineering, COMSATS University Islamabad, Wah Campus, Islamabad, Pakistan
[2]Department of Civil Engineering, College of Architecture and Environment, Sichuan University, Chengdu 610064, China
[3]Department of Civil Engineering, Universiti Teknologi PETRONAS, Seri Iskandar, Malaysia
[4]College of Architecture and Environment, Sichuan University, Chengdu 610064, China
e-mail: faisaltufail63@yahoo.com

MS received 4 June 2019; revised 4 February 2020; accepted 19 February 2020

Abstract. The use of rubber in concrete has been practiced in the engineering community for several years. However, the poor mechanical properties of rubberized concrete are a serious hurdle. This innovative research provides a closer look at improving the flexural strength of rubberized concrete beams with high rubber content using confinement technique. FRP jackets with different confinement thickness were used to recover the strength loss of rubberized concrete beams. In this paper, 66 rubberized concrete (RuC) beams having 0–50% rubber content were tested under four-point loading. RuC beams suffered up to 167% reduction in flexural strength. However, the FRP jackets were highly effective to improve the flexural strength of RuC beams. The statistical models were developed to predict the flexural strength of FRP confined rubberized concrete beams using response surface methodology (RSM). In this regard, the effect of two principle variables; unconfined strength and number of FRP layers on the flexural strength of FRP confined rubberized concrete beams was investigated. The models were found significant because the predicted and adjusted R^2 was less than 0.2 (a limit proposed by Design Expert software). The predicted and experimental results for FRP confined rubberized concrete beams were found in good agreement. The developed statistical models provide insights into the sensitivity of parameters affecting the flexural strength. The proposed models can improve the reliability of the experiments and reduces the design and analysis time.

Keywords. FRP; concrete; beams; response surface methodology; rubberized concrete.

1. Introduction

The management of scrap tires is a serious problem due to the higher production of tires. It can cause severe public health issues. It is a well-known fact that scrap tires are very difficult to recycle because of high vulcanized rubber content. Moreover, the scrap tires can trap methane and other gases resulting in a large increase in volume and catch fire easily. The rubber particles can be used in concrete as a partial replacement of aggregates that is one of the best recycling approaches. Previous studies reported advantages of rubber such as good strength and ductility. However, the mechanical properties can be seriously affected by the addition of rubber in concrete. The use of rubber in concrete is advantageous as it is environmentally friendly. Moreover, it can improve ductility and deformation capacity of concrete because of its elastic nature. The serious drawback includes a reduction in compressive and flexural strength of rubberized concrete as compared to the conventional concrete [1–5]. This reduction in mechanical properties created a hurdle for using rubberized concrete in structural engineering applications [1]. Previous studies focused on the replacement of aggregates by rubber content [1–10]. However, reduction in flexural and compressive strength was observed by the replacement of rubber content in concrete [11, 12]. There are different factors involved in this reduction such as the replacement type and properties of rubber content [13]. The addition of rubber in concrete can also yield inconsistent results as reported in the literature [11]. Poor bonding between rubber and cement paste is responsible for the reduction in compressive and flexural strength of rubberized concrete [14]. High air content is also responsible for the reduction in strength and poor mechanical properties of rubberized concrete (RuC) [15, 16]. Extensive research has been published on FRP confinement

*For correspondence
Published online: 09 May 2020

of concrete in recent years [17–22]. FRP confinement can increase the compressive and flexural strength of concrete due to the high strength and stiffness of FRP. The combination of FRP and rubberized concrete beams can improve the flexural strength and other mechanical properties of rubberized concrete.

Several types of research have been performed on FRP confinement of conventional concrete beams [23–26]. FRP jacketing can significantly improve the shear and flexural strength of conventional concrete beams. However, according to the author's knowledge, no previous research has focused on the FRP confinement of rubberized concrete. Moreover, it is important to use a powerful tool for statistical modeling that can enhance the understanding of the parameters affecting the strength of rubberized concrete beams. Statistical models can be constructed using a very useful RSM technique to develop a relationship between the input and output variables [27]. This technique can reduce the time to analyze and design the experiments without using significant effort. RSM technique can be performed with a limited number of resources and a strength model can be developed using input parameters affecting the product. The sensitivity of the input parameters can be determined which can provide useful insight into the behavior of the system [28]. Furthermore, the best possible solution can be derived using a limited number of experiments and resources. The usefulness of RSM method can be described as (a) development of output using limited resources, (b) the time required to complete the analysis and design of the experiment is very less, (c) regression models can be developed with high accuracy, and (d) the predicted and experimental values can easily be statistically validated. This technique is commonly used to design or analyze the experiments and common in the engineering community. However, its use in FRP confinement of concrete is still novel. RSM technique has been successfully used by researchers to successfully optimize and analyze the experiments [27, 29].

This research for the first time uses the RSM technique to analyze the FRP confinement of rubberized concrete beams. The experimental test results form this research will contribute to the use of FRP confined rubberized concrete as a structural material with more confidence. This paper aims to investigate the FRP confinement on rubberized concrete beams for the first time. The statistical models for FRP confined RuC beams will be developed using RSM and regression analysis. The unconfined strength, aggregate effect and confinement thickness are the main parameters of the study.

2. Experimental program

This research study is comprised of 66 rubberized concrete beams. The program was divided into three groups: (a) 0–50% fine aggregate replaced by rubber content, (b) 0–50% coarse aggregate replaced by rubber content, and (c) 50% fine and coarse aggregate replaced by rubber content coarse. The flexural strength of rubberized concrete beams was investigated and parameters were unconfined strength, aggregate effect and confinement thickness.

2.1 *Materials*

Ordinary Portland cement according to ASTM C1157 was used having 42 MPa strength, 30% fly ash and 70% pure cement by mass. Locally available fine aggregates (2.65 specific gravity) were procured from Chengdu, Sichuan province. The admixtures i.e., silica fume and fly ash were used. Water absorption, Oven dry density, specific gravity bulk density, and flakiness index were measured. Table 1 shows the physical properties of mineral aggregate and rubber content as reported in previously tested experiments by the author [30]. Figure 1 shows the particle size distribution of rubber content and mineral aggregates used in this research.

2.2 *Statistical modeling using RSM technique*

This paper uses commercial software (Design Expert) to analyze the experiments for FRP confined rubberized concrete. The relationship between input parametric variables and output factors can be established. This RSM design tool includes procedure as (a) input the parametric factors to design the experiments, (b) response is achieved after the experiments, (c) development of statistical models using input and output factors, and (d) optimization of models using the robust tool [31]. Different models can be used such as linear or quadratic according to the output requirements. These models are responsible for predicting the response such as flexural strength or other mechanical properties of the product. The flow chart for easy understanding of the response surface method is shown in figure 2. For this particular research, the quadratic model was used to develop statistical models.

2.3 *Specimen preparation*

The concrete mix was prepared as (a) the aggregate and rubber content were mixed for 30 s, (b) the water was added and mixed, (c) the additional water was poured after mixing with admixtures (Silica Fume and Fly Ash), and (d) the concrete mixture was mixed for around 3 min. In the casting procedure, the specimens were cast using two layers in a vibration table for proper compaction. The rubberized concrete beam specimens were 100 × 100 × 400 mm. The specimens were covered with sheets and were cured in a curing tank for 24 h after demoulding. Figure 3 shows the casting of rubberized concrete beams.

Table 1. Physical properties of mineral aggregate and rubber [30].

Material (size in mm)	Apparent density (g/ cm^3)	Oven dry density (g/ cm^3)	Water absorption (%)	Specific gravity	Bulk density (g/ cm^3)	Flakiness Index
Rubber (0–5)	0.78	–	–	–	0.42	–
Rubber (5–10)	1.08–1.24	1.0–1.10	4.90–7.90	1.08	0.46	6.3–7.9
Rubber (10–20)	2.60	2.54	0.78–1.26	1.08	0.48	9.8–15.5
Sand (0–5)	2.60	2.54	0.5	1.08	1.74	–
Gravel (5–10)	2.67	2.56	1.22	2.60	1.48	6.80
Gravel (10–20)	2.67	2.56	1.22	2.60	1.54	9.70

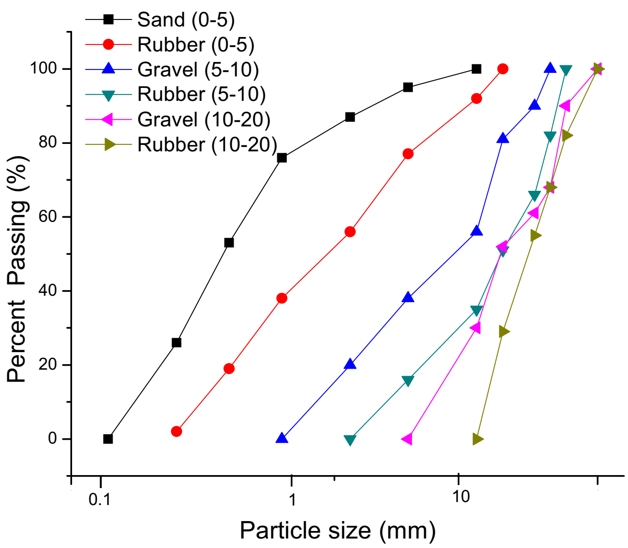

Figure 1. Particle size distribution of mineral aggregates and rubber.

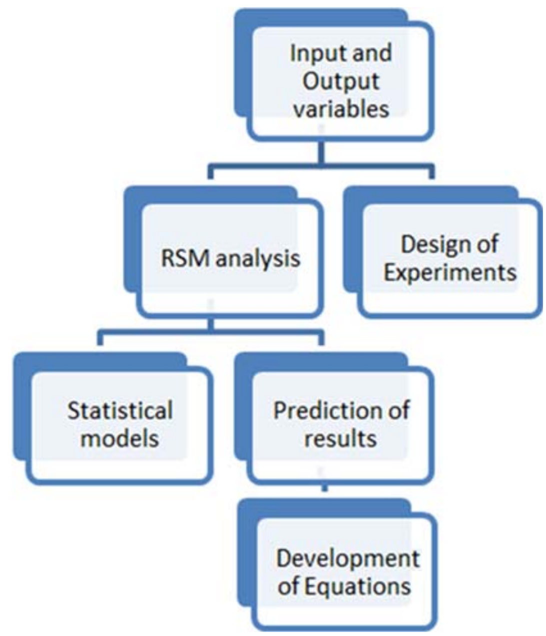

Figure 2. Response surface method approach.

Figure 3. Casting of rubberized concrete beams.

2.3a *FRP fabrication and properties*: The unidirectional FRP sheets were used to confine rubberized concrete beams. The properties of FRP with epoxy are shown in table 2. The properties of FRP and epoxy were provided by the manufacturer. The tensile strength of cured laminate (FRP and epoxy) was 894 MPa. The tensile elastic modulus and percentage elongation were 65402 and 1.7% respectively.

2.3b *Specimen confinement and test setup*: Carbon fiber reinforced polymer (CFRP) jackets with 1, 2 and 3 layers were used to confine rubberized concrete cylinders in groups 1, 2 and 3. The CFRP was wrapped on rubberized concrete beams with 50% rubber replacement levels. The experimental program consisted of 66 standard-sized rubberized concrete beams (100×100×400 mm). A total of 27 beams were wrapped with CFRP to investigate the behavior and effectiveness of FRP confinement on rubberized concrete. One, two, and three layers of FRP were used to determine the effectiveness of FRP sheets for rubberized concrete for compressive strength and deformability. Wet layup technique was used to wrap FRP sheets on rubberized concrete beams. FRP fabrication for rubberized concrete beams is shown in figure 4. The dust particles were removed from the surface of the beams before the application of FRP and epoxy. The epoxy had two components A and B, they were mixed according to the data sheet

Table 2. Properties of FRP jackets (fabric and laminate).

Property	FRP fabric	Laminate
Orientation of fibers	O^0	–
Tensile strength (MPa)	4100	894
Tensile elastic modulus (MPa)	231000	65402
Elongation (%)	1.7	1.33
Primary fiber direction	Unidirectional	–

Figure 4. Fabrication of FRP jackets.

provided by the manufacturer. The adhesive hardened after 5 h. The specimens were tested under a four-point loading test using a 300 kN capacity universal testing machine. An overlap of 100 mm for FRP jacketing was provided to avoid de-bonding and premature failure of beams. The cylinders were loading up to failure using a loading rate of 0.25 MPa/s. Figure 5 shows the general view of the test setup. Each loading segment in the test setup had round edges to accurately transfer the load from the testing machine to the concrete beams.

Figure 5. General view of the test setup.

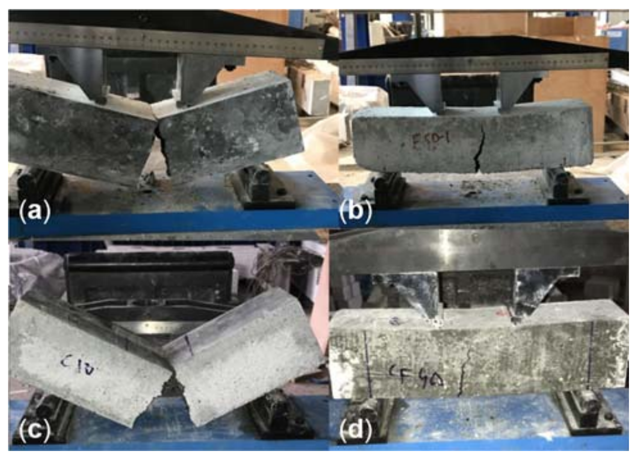

Figure 6. Failure modes of unconfined RuC beams with (a) 0% rubber, (b) 50% fine rubber, (c) 10% coarse rubber, and (d) 40% fine and coarse rubber content.

3. Results and discussion

3.1 *Failure modes*

The plain and less rubberized concrete beams containing 0–30% rubber content in all groups showed a typical failure pattern of under-reinforced concrete beams. The brittle failure was observed with vertical flexural cracks in the pure bending region. However, the cracking pattern was observed to be different in group 3 (fine and coarse rubber replacement) with high rubber content (50%), showed higher deformation and delayed cracking. Cracks initiated from mid of the beams and spread towards the supports in a gentle manner. Crack widths increased considerably after the load increased. The crack waves propagated towards the top of the beams. The failure modes of unconfined RuC beams are shown in figure 6.

The failure modes of CFRP-confined rubberized concrete were more ductile in nature as compared to the unconfined RuC cylinder. The group 3 showed delayed cracking and more ductility as compared to group 1 (fine rubber replacement) and 2 (coarse rubber replacement) with the same reinforcement ratio of FRP. A detachment of FRP in group 1 was observed as shown in figure 7. The detachment of FRP could be due to rough surface of rubber particles that decreases the effectiveness of adhesive. However, no considerable difference in failure pattern was observed with increasing layers of FRP. Overall, FRP successfully

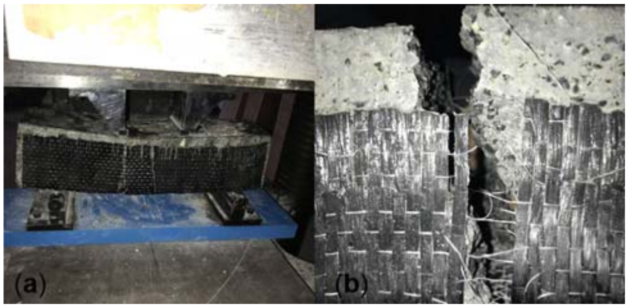

Figure 7. The typical failure mode of CFRP-confined RuC beams (a) 50% fine and coarse rubber, (b) detachment of FRP from RuC beam (50% fine rubber).

delayed the onset of cracking and reduced the brittle nature of concrete beams.

3.2 *Aggregate effect on flexural strength of rubberized concrete beams*

Table 3 shows the flexural strength of unconfined RuC beams. Equation 1 was used to calculate the flexural strength of concrete beams.

$$\sigma = \frac{FL}{bd^2} \quad (1)$$

Where б = Flexural stress (MPa), L = length of the span in (mm)

F = load (N)

b = width of the beam (mm)

d = depth of the beam (mm)

The rubberized concrete mixes BF-10, BF-30 and BF-50 achieved 5.1, 4.44 and 2.43 MPa flexural strength. Strength reduction of 8.2, 24.3 and 127.2% was observed for 10, 30 and 50% replacement levels of rubber content in the concrete mix. The mix BF-50 showed the highest reduction in flexural strength with 50% rubber content. The flexural strength of rubberized concrete beams was compared with the existing literature [10, 32]. The comparison between the predicted and experimental flexural strength shows variation in results with the same rubber content in concrete. The reason is attributed to different sources and nature of rubber content. The specimen BC-10, BC-30 and BC-50 achieved 4.86, 3.93 and 2.4 MPa flexural strength. Strength reduction of 8.2, 24.3 and 127.2% was observed for 10, 30, and 50% replacement levels of rubber content in the concrete mix. The predicted results by Moh *et al* were close to the experimental test values in this group. The mix BC-50

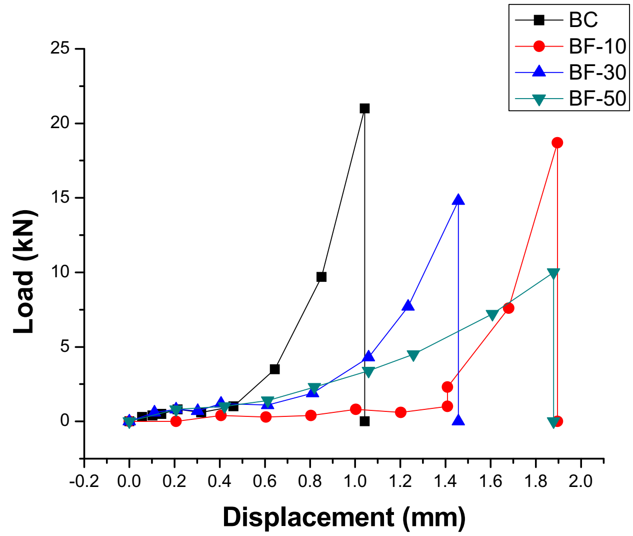

Figure 8. Load displacement curves of CFRP-confined rubberized concrete beams (Group-1).

Table 3. Flexural Strength of rubberized concrete beams.

ID	Ultimate failure load P_u (kN)	Unconfined flexural strength Exp (MPa)	Predicted Batayneh *et al* (MPa)	Predicted Moh *et al* (MPa)	Flexural strength reduction (%)
C	21	5.52	5.52	5.52	–
BF-10	18.7	5.1	4.59	4.896	8.2
BF-30	14.80	4.44	2.886	3.33	24.3
BF-50	10	2.43	1.215	1.3365	127.2
BC-10	16	4.86	4.374	4.6656	8.2
BC-30	13.1	3.93	2.5545	2.9475	24.3
BC-50	10.5	2.4	1.2	1.32	127.2
BCF-50	6.8	2.07	1.5111	1.656	167

showed a more pronounced reduction in strength with 50% rubber content. The recorded flexural strength of rubberized concrete mix BCF-50 was 2.07 kN. The strength reduction of 167% was observed for 50% replacement levels of rubber content in the concrete mix. The mix BCF-50, similar to group 1 and 2, showed a higher reduction in strength with 50% rubber content. The flexural strength prediction by Moh *et al* was close to the experimental test results in this group.

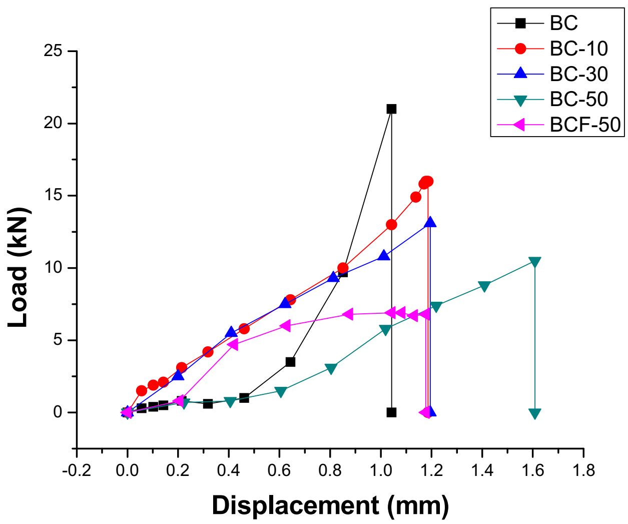

Figure 9. Load displacement curves of CFRP-confined rubberized concrete beams (group 2 and 3).

The addition of rubber resulted in reduced strength of RuC beams as compared to conventional concrete beams. The results of fine, coarse, and combined fine and coarse aggregate replacement by rubber content are shown in table 3. A percentage reduction of 8–127% in compressive strength was observed for fine rubber replacement in RuC. The mix BF-50 showed the highest reduction in compressive strength with 50% rubber content in group 1. It is worth mentioning that the addition of rubber content in concrete leads to early cracking and premature crack formation. These factors lead to low ultimate strength for rubberized concrete beams. Higher reduction in strength compressive strength was recorded in the mixes with coarse aggregate replacement as compared to the fine rubber replaced counterparts. A reduction of compressive strength up to 130% was recorded for coarse aggregate replacement in RuC (group 2). The highest percentage loss in strength was observed for 50% rubber replacement in the mix (BC-50). The strength loss in the range of 14–130% was observed for coarse aggregate replacement with rubber content in RuC. The decrease in compressive strength was slightly more pronounced for coarse aggregate replacement by rubber content over the corresponding fine aggregate replaced RuC. The highest reduction in strength was

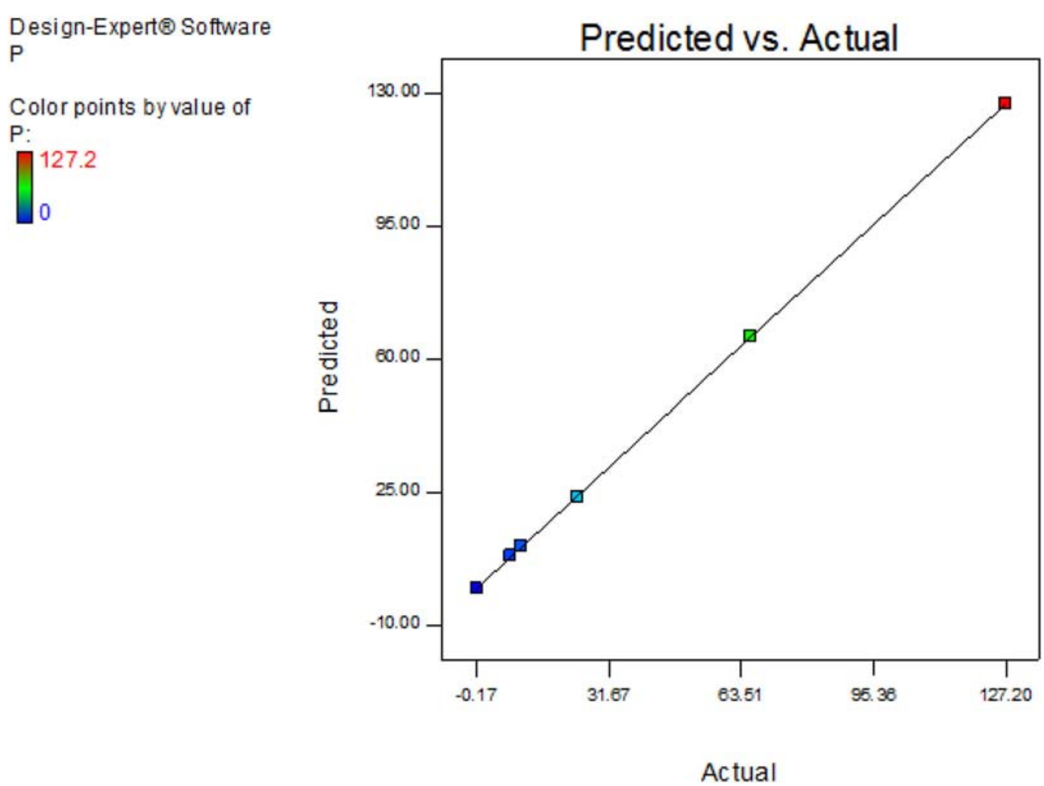

Figure 10. Predicted versus actual results by RSM (Group-1).

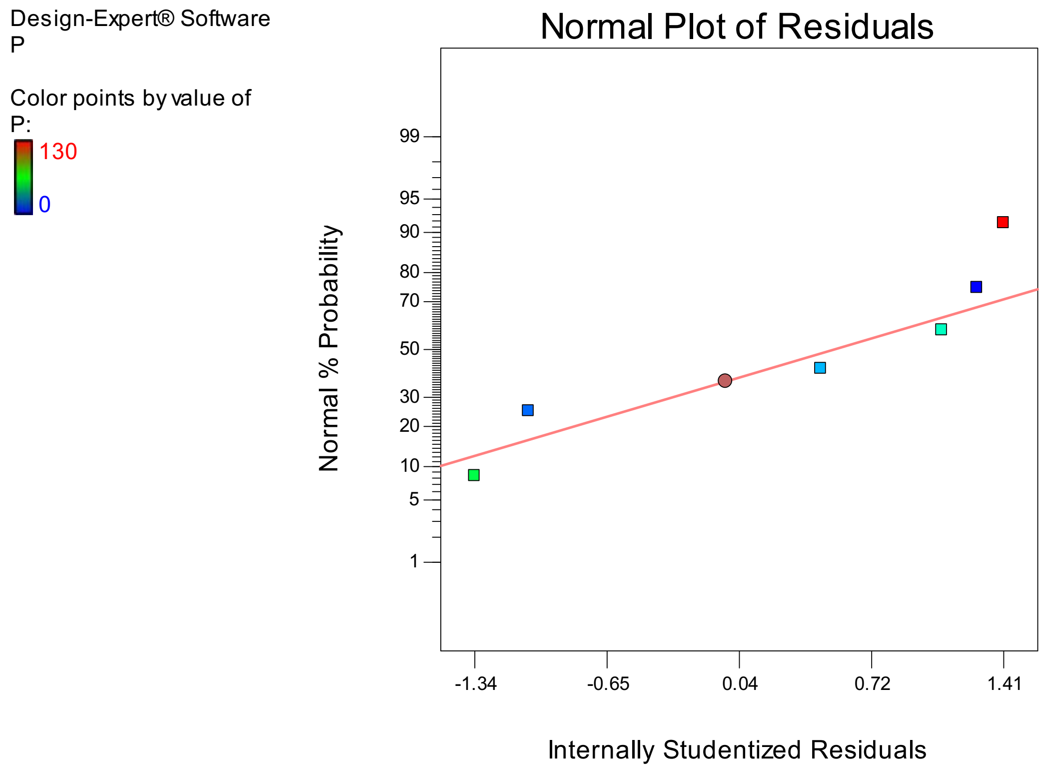

Figure 11. Predicted versus actual results by RSM (Group-2).

Table 4. Analysis of variance table (ANOVA) for response surface quadratic model (G-1).

Source	Sum of Squares	df	Mean Square	F value
Model	11977.24	3	3992.41	24270.80
x-Unconfined Strength (kN)	3094.63	1	3094.63	18812.99
x^2	120.65	1	120.65	733.45
x^3	23.32	1	23.32	141.77

Table 5. Analysis of variance table (ANOVA) for response surface quadratic model (G-2).

Source	Sum of squares	df	Mean square	F value
Model	10830.00	3	3610.00	32006.86
A-fc' (kN)	4401.85	1	4401.85	39027.54
A^2	111.20	1	111.20	985.96
A^3	19.49	1	19.49	172.80

observed for combined fine and coarse rubber replacement in RuC (group 3). The reduction in strength up to 167% was recorded in this group i.e., higher than the group 1 and 2. The highest reduction in strength was observed for the mix (BCF-50), where the mineral aggregate in concrete was replaced with a combined 50% fine and coarse rubber content. Rubberized concrete shows higher lateral dilation than conventional concrete. The rubber particles also show higher lateral dilation when subjected to loading [33, 34].

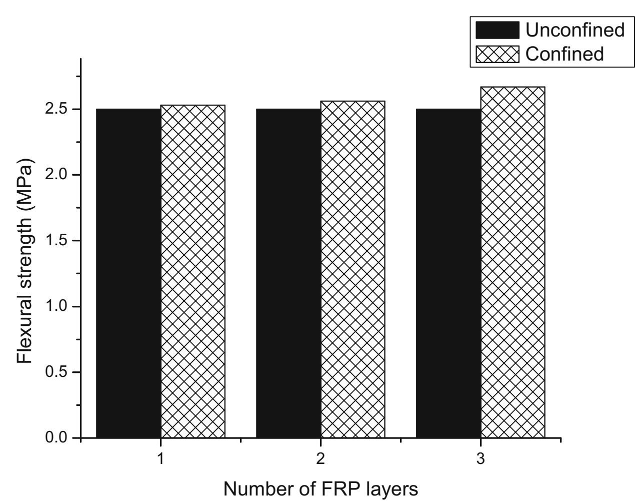

Figure 12. Load carrying capacity of CFRP-confined rubberized concrete beams (Group-1).

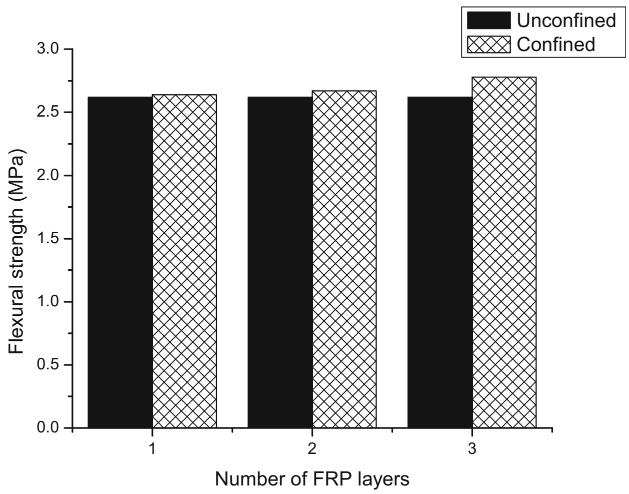

Figure 13. Load carrying capacity of CFRP-confined rubberized concrete beams (Group-2).

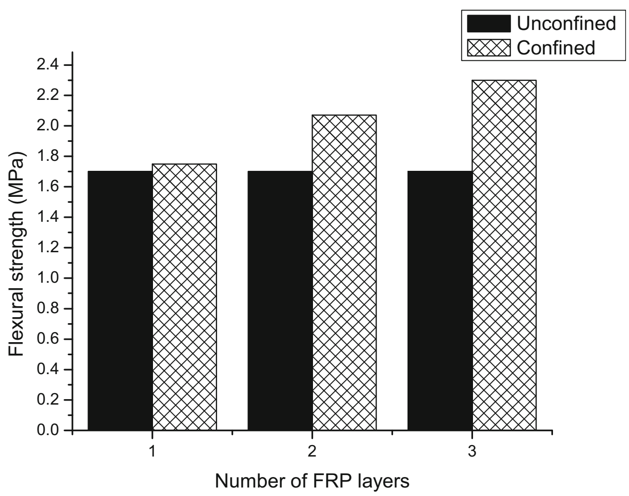

Figure 14. Load carrying capacity of CFRP-confined rubberized concrete beams (Group-3).

This phenomenon produces higher tensile stresses near rubber content in concrete. The load displacement curves for unconfined RuC are shown in figures 8 and 9. Figures 10 and 11 show the predicted versus recorded test results for unconfined RuC for groups 1 and 2. The parametric variable factor for this statistical model was the percentage of rubber content. Tables 4 and 5 show the theoretical versus experimental results for groups 1 and 2. The output response parameter for this model was the percentage axial compressive strength loss in RuC. The predicted and recorded test values were in good agreement because the value of R^2 was less than 1. The regression equations 1 and 2 were developed to predict the reduction in strength of rubberized concrete beams in groups 1 and 2. The statistical graph for RuC with both fine and coarse rubber replacement was not plotted. The reason was less number of parametric values for percentage rubber

Table 6. CFRP-confined RuC (flexural strength).

ID	Unconfined flexural strength (MPa)	Confined flexural strength (MPa)	Confinement ratio
BF-50FRP1L	2.50	2.53	1.01
BF-50FRP2L	2.50	2.56	1.02
BF-50FRP3L	2.50	2.67	1.06
BC-50FRP1L	2.62	2.64	1.00
BC-50FRP2L	2.62	2.67	1.01
BC-50FRP3L	2.62	2.78	1.06
BCF-50FRP1L	1.70	1.75	1.02
BCF-50FRP2L	1.70	2.07	1.21
BCF-50FRP3L	1.70	2.30	1.35

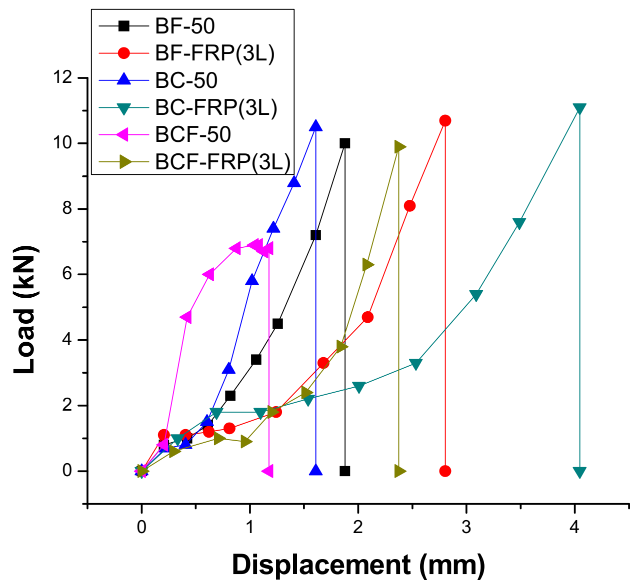

Figure 15. Load displacement curves of unconfined and CFRP-confined rubberized concrete beams.

replacement in that group. Equations 2 and 3 were developed for groups 1 and 2.

$$P = 84.89 - 170.24f'_c + 131.43f'^2_c - 50.02f'^3_c \quad (2)$$

$$P = 85.32 - 169.77f'_c + 129.44f'^2_c - 48.82f'^3_c \quad (3)$$

Where P and fc' are percentage reduction in strength and unconfined strength respectively.

3.3 *Effect of confinement thickness and unconfined strength on FRP-confined rubberized concrete beams*

The test results of CFRP confined rubberized concrete beams are indicated in figures 12, 13 and 14. The confined

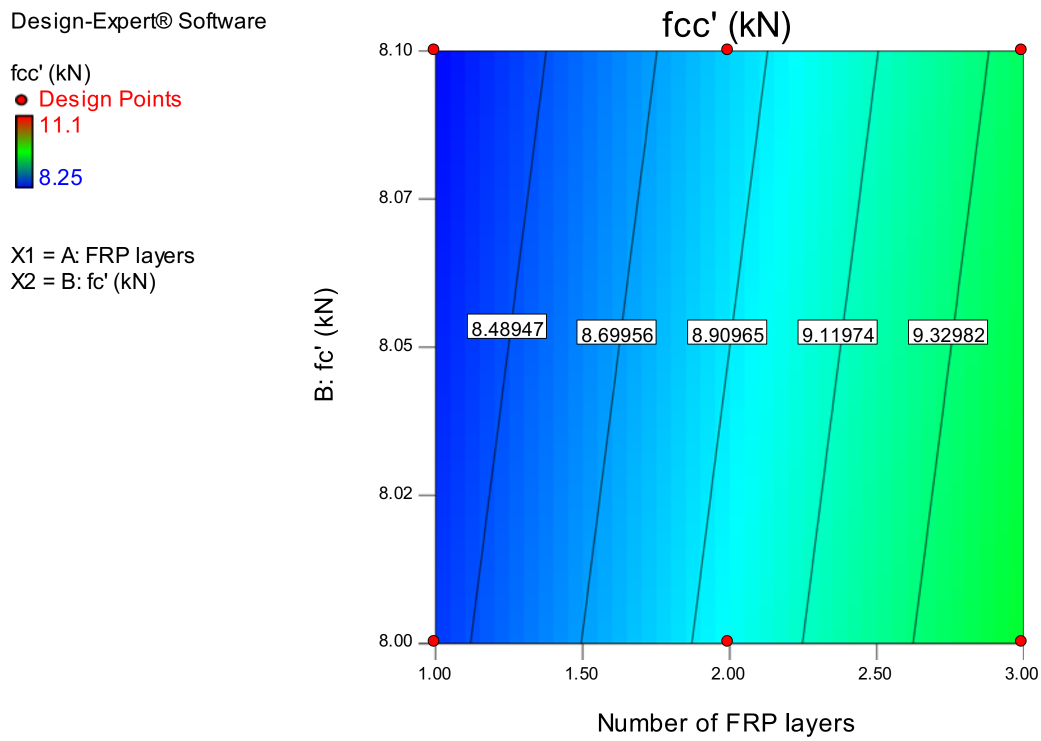

Figure 16. Contour plot of FRP confined rubberized concrete beams (RSM technique).

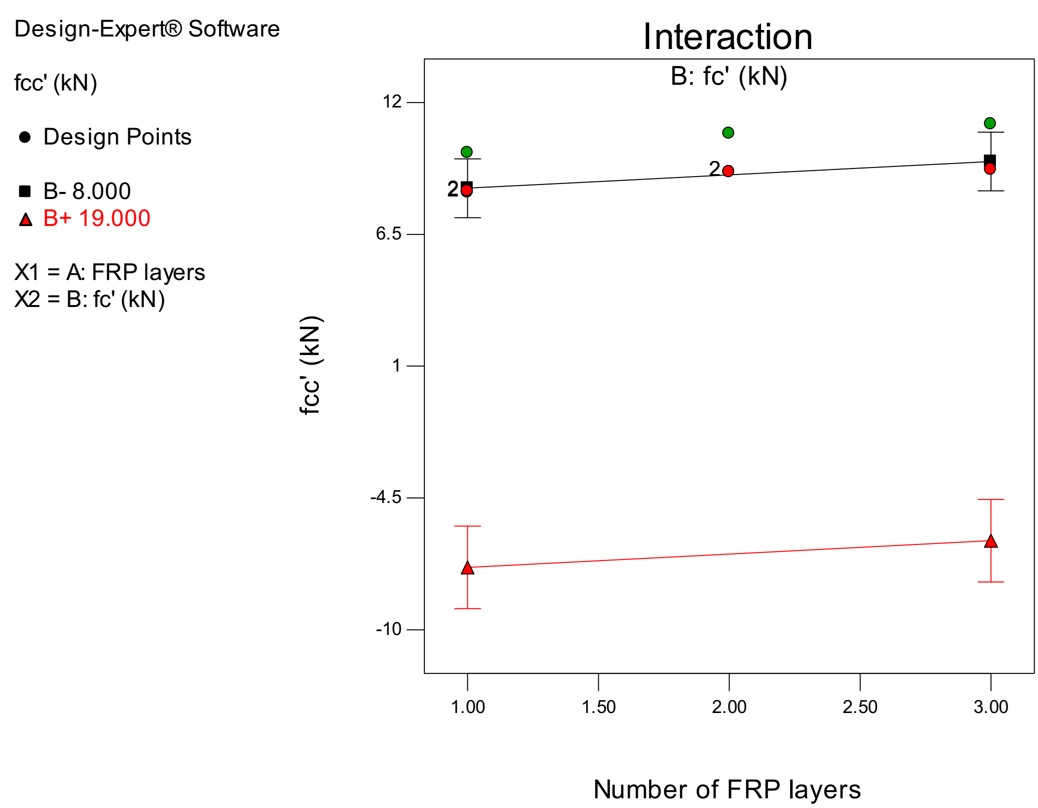

Figure 17. Interaction diagram of FRP confined rubberized concrete beams (RSM).

flexural strength of 2.53, 2.56 and 2.67 MPa was reported for mixes BF-50FRP1L, BF-50FRP2L, and BF-50FRP3L respectively. The confinement ratios were 1.01, 1.02 and 1.07 for 1, 2 and 3 layers of CFRP confinement. Strength increment of 2, 3 and 7% were recorded for 1, 2 and 3 layers of CFRP-confined rubberized concrete over the unconfined RuC. The confined compressive strength of 2.64, 2.67 and 2.78MPa was reported for mixes BC-50FRP1L, BC-50FRP2L, and BC-50FRP3L respectively. The confinement ratios were 1.00, 1.02 and 1.06 for 1, 2 and 3 layers of CFRP confinement. Strength increment of 0.64, 1.8 and 5.71% was recorded for 1, 2 and 3 layers of CFRP-confined rubberized concrete over the unconfined RuC. The test results of CFRP confined rubberized concrete beams are summarized in table 6. The confined compressive strength of 1.75, 2.075 and 2.30 MPa was recorded for mixes BCF-50FRP1L, BCF-50FRP2L, and BCF-50FRP3L respectively. The confinement ratios were 1.02, 1.22 and 1.35 for 1, 2 and 3 layers of CFRP confinement. Strength increment of 2.9, 22.05 and 35.29% was recorded for 1, 2 and 3 layers of CFRP-confined rubberized concrete over the unconfined RuC. It is worth highlighting that Group 3 was superior to group 1 and 2 in terms of gain in strength by using CFRP confinement on rubberized concrete beams. Figure 15 shows the load displacement curves for CFRP confined rubberized concrete beams and its comparison with unconfined beams.

The effect of fc' (unconfined compressive strength of concrete) and a number of FRP layers on the compressive strength of FRP confined-RuC beams is investigated. The addition of rubber content resulted in reduced strength of rubberized concrete beams. The jacketing of rubberized concrete (RuC) by FRP recovered and further enhanced the strength of rubberized concrete beams. Strength increment of 2.9, 22.05 and 35.29% was recorded for 1, 2 and 3 layers of CFRP-confined rubberized concrete beams over the unconfined RuC. The RSM technique was employed to investigate the effect of parameters (a) effect of unconfined axial compressive strength and (b) number of FRP layers on strength enhancement for FRP confined RuC beams. The statistical parametric comparison (contour plot) for strength enhancement of FRP confined RuC beams is shown in figure 16. The graphs were plotted using the response surface method (RSM). The obtained

Table 7. Analysis of variance table (ANOVA) for response surface quadratic model.

Source	Sum of squares	df	Mean square	F value	p-value
Model	1.17	2	0.58	11.98	0.0371
A-FRP layers	1.16	1	1.16	23.74	0.0165
B-fc' (kN)	0.010	1	0.010	0.21	0.6752
Residual	0.15	3	0.049	–	–
Model	1.17	2	0.58	11.98	0.0371

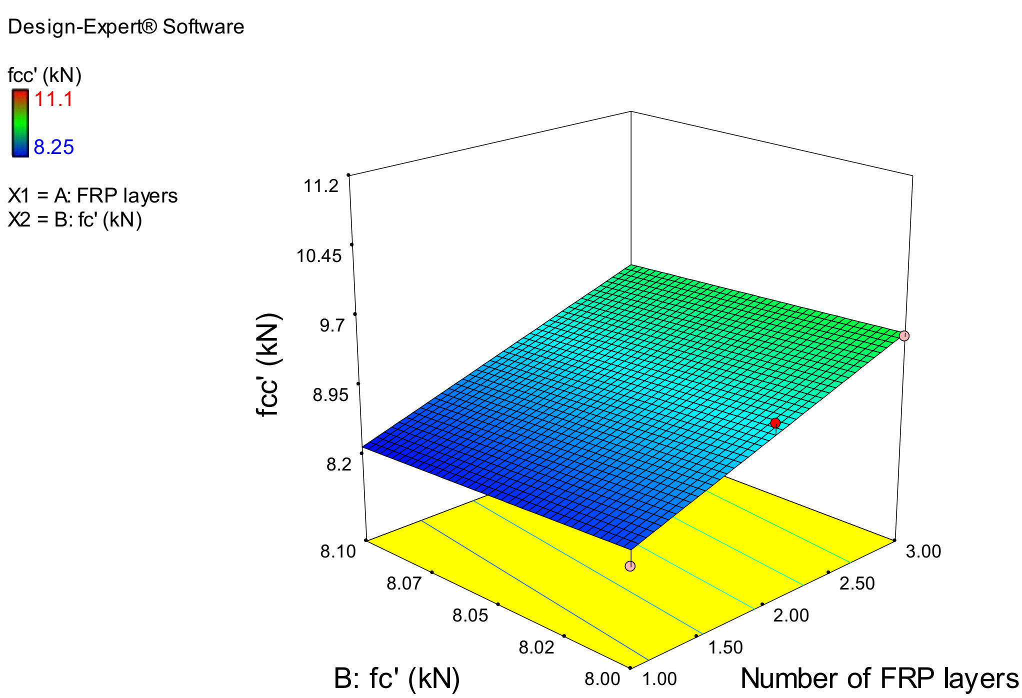

Figure 18. 3D plot of FRP confined rubberized concrete beams (RSM technique).

models show a reliable correlation between the response and parametric factors. The interaction plot shown in figure 17 depicts how the factors collaborate for the output response. These statistical models reveal that the unconfined strength (fc') highly affects the CFRP-confined strength of rubberized concrete beams and is a highly sensitive factor. Analysis of variance table (ANOVA) for the response factor is shown in table 7. The regression equation "fcc' = 4.37 + 0.54 n−4.58fc'" from the statistical model was developed. Confined strength is designated by the response factor fcc'. The parametric factors fc' and n show the unconfined concrete compressive strength and number of FRP layers respectively. The 3D diagram of two parametric factors and a response factor involved in the statistical model are depicted in figure 18.

4. Conclusions

This research for the first time investigates the FRP confinement of rubberized concrete beams. RSM technique was utilized to develop statistical models and analyze the experiments. The principle variables utilized in this research were confinement thickness and unconfined strength. The following conclusions were drawn from this research.

- FRP successfully delayed the onset of cracking and reduced the brittle nature of concrete beams. The failure modes of CFRP-confined rubberized concrete were more ductile in nature as compared to the unconfined RuC cylinder.
- The RuC beams suffered flexural strength reduction up to 167% with 50% rubber content.
- The highest reduction in flexure strength was observed for combined fine and corase aggregate replacement with rubber content in RuC beams. The inclusion of rubber content in concrete resulted in premature microcracking.
- CFRP jacketing enhanced the flexural strength up to 35% of unconfined rubberized concrete beams. Batayneh's model was close to the experimental results for predicting the flexural strength of RuC beams.
- The statistical models revealed that the unconfined strength (fc') highly affects the CFRP-confined strength of rubberized concrete beams and is a highly sensitive factor.

5. Recommendations

Further research should be directed towards the durability of rubberized concrete for practical engineering applications. Moreover, the usage of rubberized concrete in extreme weather conditions in long term should also be evaluated.

Nomenclature/notations

b	Width of the beam (mm)
d	depth of the beam (mm)
F	load (N)
fc'	unconfined compressive strength of concrete
fcc'	FRP-confined compressive strength of concrete
σ̄	flexural stress (MPa)
L	length of the span in (mm)
n	number of FRP layers

References

[1] Raffoul S, Garcia R, Escolano-Margarit D, Guadagnini M, Hajirasouliha I and Pilakoutas K 2017 Behaviour of unconfined and FRP-confined rubberised concrete in axial compression. *Constr. Build. Mater.* 147: 388–397.

[2] Thomas B S and Gupta R C 2016 A comprehensive review on the applications of waste tire rubber in cement concrete. *Renew. Sustain. Energy Rev.* 54: 1323–1333.

[3] Sengul O 2016 Mechanical behavior of concretes containing waste steel fibers recovered from scrap tires. *Constr. Build. Mater.* 122: 649–658.

[4] Huang S-S, Angelakopoulos H, Pilakoutas K and Burgess I 2016 Reused tyre polymer fibre for fire-spalling mitigation. *Appl. Struct. Fire Eng.*

[5] Goulias D G and Ali A-H 1998 Evaluation of rubber-filled concrete and correlation between destructive and nondestructive testing results. *Cem. Concr. Aggreg.* 201: 140–144.

[6] Son K S, Hajirasouliha I and Pilakoutas K 2011 Strength and deformability of waste tyre rubber-filled reinforced concrete columns. *Constr. Build. Mater.* 25: 218–226.

[7] Liu F, Zheng W, Li L, Feng W and Ning G 2013 Mechanical and fatigue performance of rubber concrete. *Constr. Build. Mater.* 47: 711–719.

[8] Xue J and M Shinozuka 2013 Rubberized concrete: A green structural material with enhanced energy-dissipation capability. *Constr. Build. Mater.* 42: 196–204.

[9] Najim K B and Hall M R 2012 Mechanical and dynamic properties of self-compacting crumb rubber modified concrete. *Constr. Build. Mater.* 27: 521–530.

[10] Batayneh M K, Marie I and Asi I 2008 Promoting the use of crumb rubber concrete in developing countries. *Waste Manag.* 28: 2171–2176.

[11] Youssf O, Hassanli R and Mills J E 2017 Mechanical performance of FRP-confined and unconfined crumb rubber concrete containing high rubber content. *J. Build. Eng.* 11: 115–126.

[12] Youssf O, ElGawady M A and Mills J E 2015 Experimental investigation of crumb rubber concrete columns under seismic loading. In: *Structures*. Elsevier.

[13] Youssf O, Mills J E and Hassanli R 2016 Assessment of the mechanical performance of crumb rubber concrete. *Constr. Build. Mater.* 125: 175–183.

[14] Hernandez-Olivares F, Barluenga G, Bollati M and Witoszek B 2002 Static and dynamic behaviour of recycled tyre rubber-filled concrete. *Cem. Concr. Res.* 3210: 1587–1596.

[15] Richardson A E, Coventry K A and Ward G 2012 Freeze/thaw protection of concrete with optimum rubber crumb content. *J. Clean. Prod.* 23: 96–103.

[16] Sukontasukkul P 2009 Use of crumb rubber to improve thermal and sound properties of pre-cast concrete panel. *Constr. Build. Mater.* 23: 1084–1092.

[17] Ozbakkaloglu T and Idris Y 2014 Seismic behavior of FRP-high-strength concrete–steel double-skin tubular columns. *J. Struct. Eng.* 140: 04014019.

[18] Youssf O, ElGawady M A and Mills J E 2015 Displacement and plastic hinge length of FRP-confined circular reinforced concrete columns. *Eng. Struct.* 101: 465–476.

[19] Youssf O, ElGawady M A and Mills J E 2016 Static cyclic behaviour of FRP-confined crumb rubber concrete columns. *Eng. Struct.* 113: 371–387.

[20] Youssf O, ElGawady M A, Mills J E and Ma X 2014 Finite element modelling and dilation of FRP-confined concrete columns. *Eng. Struct.* 79: 70–85.

[21] Liu J and Sheikh S A 2013 Fiber-reinforced polymer-confined circular columns under simulated seismic loads. *ACI Struct. J.* 110.

[22] Hassanli R, Youssf O, and Mills J E 2017 Seismic performance of precast posttensioned segmental FRP-confined and unconfined crumb rubber concrete columns. *J. Compos. Constr.* 21: 04017006.

[23] Naaman A and Jeong S 2004 Structural ductility of concrete beams prestressed with FRP tendons. In: *Non-Metallic (FRP) Reinforcement for Concrete Structures: Proceedings of the Second International RILEM Symposium*. CRC Press.

[24] Triantafillou T C 1998 Shear strengthening of reinforced concrete beams using epoxy-bonded FRP composites. *ACI Struct. J.* 95: 107–115.

[25] Theriault M and Benmokrane B 1998 Effects of FRP reinforcement ratio and concrete strength on flexural behavior of concrete beams. *J. Compos. Constr.* 2: 7–16.

[26] Toutanji H A and Gomez W 1997 Durability characteristics of concrete beams externally bonded with FRP composite sheets. *Cem. Concr. Compos*. 19: 351–358.

[27] Zahid M, Shafiq N, Isa M H and Gil L 2018 Statistical modeling and mix design optimization of fly ash based engineered geopolymer composite using response surface methodology. *J. Clean. Prod.* 194: 483–498.

[28] Anderson M and Whitcomb P 2002 *Find the Optimal Formulation for Mixtures.* Stat-Ease Inc, Minneapolis.

[29] Zahid M, Shafiq N and Jalal A 2018 Investigating the effects of solarcure curing method on the compressive strength, microstructure and polymeric reaction of fly ash based geopolymer. *Constr. Build. Mater.* 181: 227–237.

[30] Feng X, Tufail R F and Zahid M 2019 Experimental investigation and statistical modeling of FRP confined RuC using response surface methodology. *Civ. Eng. J.* 5: 268–283.

[31] Son D, Lee J, Qiao S, Ghaffari R, Kim J and Lee J E 2014 Multifunctional wearable devices for diagnosis and therapy of movement disorders. *Nat. Nanotechnol.* 9: 397.

[32] Mohammed B S, Hossain K M A, Swee J T E, Wong G and Abdullahi M 2012 Properties of crumb rubber hollow concrete block. *J. Clean. Prod.* 23: 57–67.

[33] Gholampour A, Ozbakkaloglu T and Hassanli R 2017 Behavior of rubberized concrete under active confinement. *Constr. Build. Mater.* 138: 372–382.

[34] Youssf O, ElGawady M A, Mills J E and Ma X 2013 Experimental and finite element investigation of rubberized concrete confined by FRP. *Arinex*.